

NANO EXPRESS

Open Access

Color-tunable properties of Eu³⁺- and Dy³⁺-codoped Y₂O₃ phosphor particles

Timur Sh Atabaev^{1*}, Yoon-Hwae Hwang^{2*} and Hyung-Kook Kim^{2*}

Abstract

Rare-earth phosphors are commonly used in display panels, security printing, and fluorescent lamps, and have potential applications in lasers and bioimaging. In the present study, Eu³⁺- and Dy³⁺-codoped uniform-shaped Y₂O₃ submicron particles were prepared using the urea homogeneous precipitation method. The structure and morphology of the resulting particles were characterized by X-ray diffraction, field emission scanning electron microscope, and field emission transmission electron microscope, whereas their optical properties were monitored by photoluminescence spectroscopy. The room-temperature luminescence color emission of the synthesized particles can be tuned from red to yellow by switching the excitation wavelength from 254 to 350 nm. The luminescence intensities of red and yellow emissions could be altered by varying the dopant concentration. Strong quenching was observed at high Eu³⁺ and Dy³⁺ concentrations in the Y₂O₃ host lattice.

Keywords: Y₂O₃ particles, Luminescence, Urea homogeneous precipitation, Eu³⁺ and Dy³⁺ codoped

Background

The development of novel luminescent phosphor materials with a controllable size and morphology has been a major focus in the field of photonics and optoelectronics [1]. Phosphor nanocrystals are exceptionally promising materials in many fields of technology including photonics, luminescent displays, fluorescent lamps, lasers, cathodoluminescence, and biotechnology [2]. Moreover, the emission wavelength of rare-earth-doped nanoparticles is independent of the particle size and depends only on the dopant type, leading to lower synthesis cost. They also offer excellent chemical stability as well as high quantum yield. Different methods have been used to fabricate nanocrystalline phosphor particles, such as flame spray pyrolysis [3], co-precipitation method [4], sol-gel method [5], and solvothermal method [5]. The urea homogeneous precipitation method was recognized to be a green route for the high-yield mass production of spherical ceramic submicron particles with controllable sizes. Spherical-shaped particles can improve the optical

performance due to the high packing density and reduction of light scattering [6].

Yttrium oxide (Y₂O₃) has been investigated widely as a host material for rare-earth (RE) ion doping in optical applications [3,4,6,7] on account of its excellent chemical stability, broad transparency range (0.2 to 8 μm) with a band gap of 5.6 eV, high refractive index, and low phonon energy [1]. Furthermore, the similarities in the chemical properties and ionic radius of RE ions and Y₂O₃ make it an attractive choice as a host material [6,8].

The color tunability of yttria-based phosphors can be achieved by codoping the host material with some specific rare-earth elements. For example, in our previous report we investigated the color-tunability effect of Eu³⁺- and Tb³⁺-codoped Y₂O₃ submicron particles [8]. We showed that the color emission of synthesized particles could be tuned precisely from red to green by a simple variation of the Tb/Eu ratio and excitation wavelength. Strong energy transfer (ET) from Tb to Eu ions was observed in Tb/Eu-codoped Y₂O₃ submicron particles, but back ET from Eu³⁺ to Tb³⁺ was not significant. Ishiwada et al. investigated the Tb/Tm-codoped Y₂O₃ phosphor for high-temperature thermometry application [9]. The synthesized Tb/Tm-codoped Y₂O₃ phosphor showed a distinct change of visible emission colors from

* Correspondence: atabaev@snu.ac.kr; yhwang@pusan.ac.kr; hkkim@pusan.ac.kr

¹Department of Physics and Astronomy, Seoul National University, Seoul 151-747, Republic of Korea

²Department of Nanomaterials Engineering and BK21 Nano Fusion Technology Division, Pusan National University, Miryang 627-706, Republic of Korea

green to blue with increasing temperature. Therefore, research into Y_2O_3 codoped with other different RE activators is important because the color-tunable properties can be used in a wide range of applications. Although many studies have examined the optical properties of RE ion-doped Y_2O_3 phosphors, only a few have investigated the codoping of two or more different ions in the same yttria host material [6,8,9].

In recent years, the Eu/Dy codoping in a single host material has attracted a great deal of attention and has been extensively investigated. For example, the SrAl_2O_4 host material codoped with Eu^{3+} and Dy^{3+} is known as a new generation long-lasting luminescent phosphor material [10]. It is well known that Eu^{3+} doping into Y_2O_3 host material results in a red emission, whereas doping with Dy^{3+} results in blue-yellow emission [11]. To the best of the authors' knowledge, there are no reports of an Y_2O_3 phosphor codoped with Eu^{3+} and Dy^{3+} . In addition, there is an optimum concentration of dopant ions for all RE phosphors, but the optimum concentration also depends on several parameters, such as the size of the phosphors and synthetic route.

In the present study, urea homogeneous precipitation synthesis method was used for the preparation of Eu^{3+} - and Dy^{3+} -codoped Y_2O_3 submicron particles. The morphology and particles characteristics were investigated by X-ray diffraction (XRD), field emission

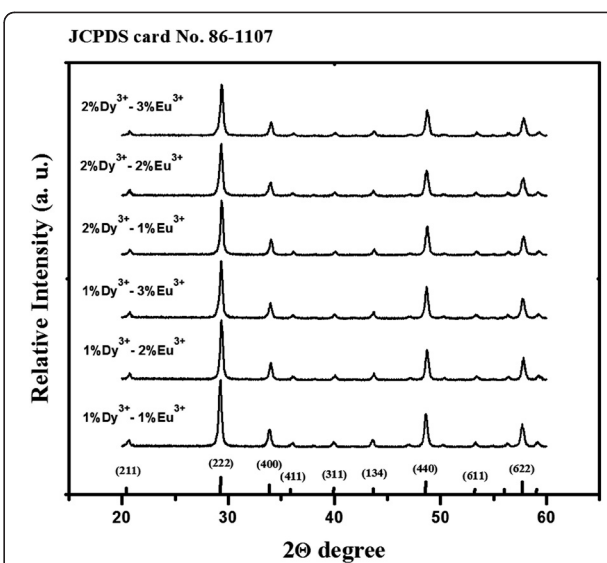


Figure 2 X-ray diffraction patterns of Y_2O_3 phosphor particles. The Y_2O_3 particles are codoped with different RE ion (Eu^{3+} and Dy^{3+}) concentrations ($T_{\text{cal.}} = 1,000^\circ\text{C}$).

scanning electron microscopy (FESEM), field emission transmission electron microscopy (FETEM), and energy dispersive X-ray (EDX) spectroscopy. The optical properties of the synthesized particles were explored by photoluminescence spectroscopy (PL). Y_2O_3 submicron particles with different concentrations of codoped Eu^{3+} and Dy^{3+} were investigated, and the luminescence intensity of these particles were found to be strongly dependent on the activators concentration. The emission color of the Eu^{3+} - and Dy^{3+} -codoped Y_2O_3 particles could be switched from red to yellow by variation of the excitation wavelength.

Methods

Chemical synthesis

Analytical grade Y_2O_3 (99.9%), europium oxide (Eu_2O_3 ; 99.9%), dysprosium oxide (Dy_2O_3 ; 99.9%), nitric acid (HNO_3 ; 70%), and urea (99% to 100.5%) were purchased from Sigma-Aldrich Corporation (MO, USA) and were used without further purification.

Uniform-shaped sub-micron Eu^{3+} - and Dy^{3+} -codoped Y_2O_3 particles were synthesized according to the reported protocols [6,8]. Phosphor precipitates were prepared by heating the corresponding RE nitrates (0.001 mol each sample) in aqueous solution of urea (40 ml H_2O and 0.5 g urea). The concentration of Eu^{3+} varied between 1 to 3 mol%, whereas the Dy^{3+} concentration varied from 1 to 2 mol%.

Physical characterization

The structure of the prepared powders was examined by XRD using a Bruker D8 Discover diffractometer (Bruker

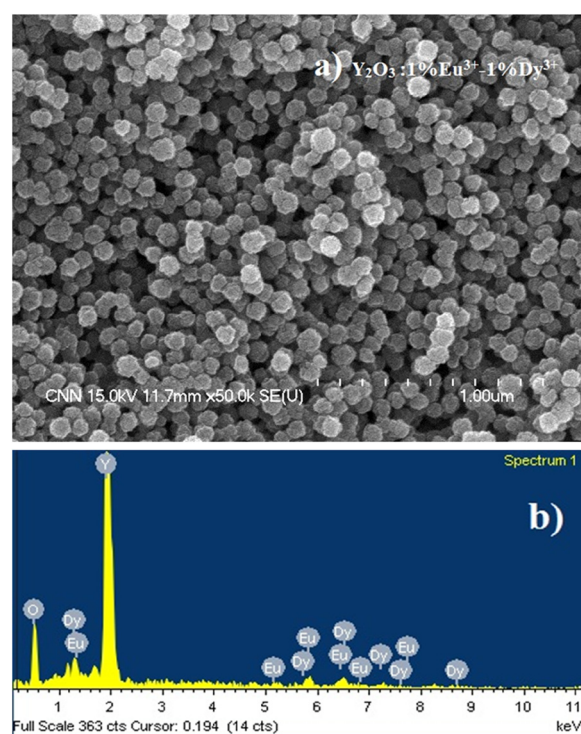


Figure 1 $\text{Y}_2\text{O}_3: 1\%\text{Eu}^{3+}-1\%\text{Dy}^{3+}$ phosphor particles ($T_{\text{cal.}} = 1,000^\circ\text{C}$). FESEM image (a) and EDX spectra (b).

Table 1 Calculated mean crystallite sizes of Eu³⁺- and Dy³⁺-codoped Y₂O₃ particles

1Dy/1Eu	1Dy/2Eu	1Dy/3Eu	2Dy/1Eu	2Dy/2Eu	2Dy/3Eu
36.42 ± 0.11	36.72 ± 0.09	36.96 ± 0.10	36.67 ± 0.14	37.01 ± 0.16	37.28 ± 0.07

Optics Inc., MA, USA) with Cu K α radiation ($\lambda = 0.15405$ nm) and a 2θ scan range of 20 to 60°. The structural properties were also analyzed using Fourier transform infrared spectroscopy (Jasco FT/IR6300, JASCO Corp., Easton, MD, USA). The morphologies of the particles were characterized by FESEM (Hitachi S-4700, Hitachi, Ltd., Tokyo, Japan) and FETEM (JEOL JEM-2100F, JEOL Ltd., Tokyo, Japan). Elemental analysis was carried out by EDX (Horiba 6853-H, HORIBA Jobin Yvon Inc., Edison, NJ, USA). The PL measurements were performed with a Hitachi F-7000 spectrophotometer equipped with a 150-W xenon lamp as an excitation source. All the measurements were performed at room temperature.

Results and discussion

Morphology and structure

The luminescence intensity depends strongly on the phosphor crystallinity [6,11]. Therefore, all synthesized particles were calcined at the temperature of 1,000°C. The morphology of the synthesized phosphor particles

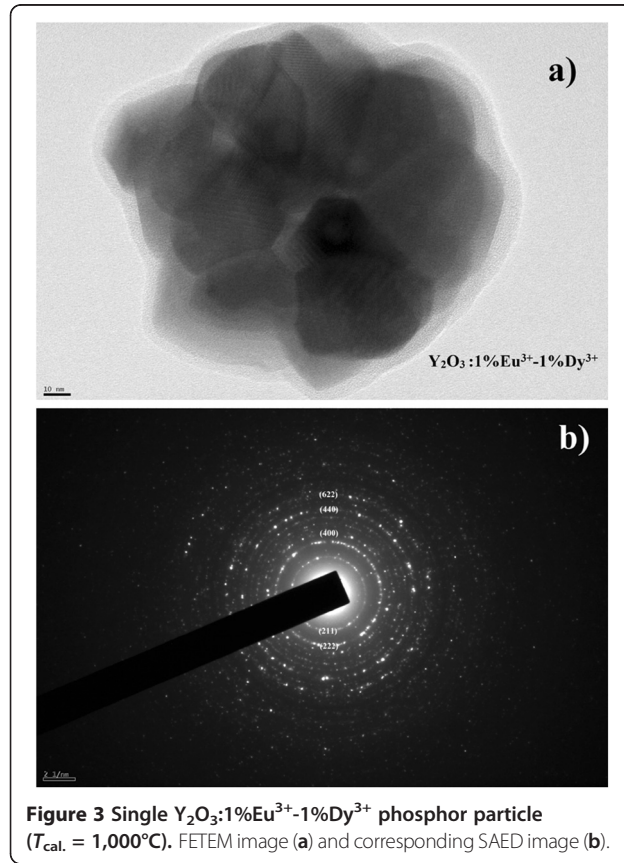


Figure 3 Single Y₂O₃:1%Eu³⁺-1%Dy³⁺ phosphor particle ($T_{\text{cal.}} = 1,000^\circ\text{C}$). FETEM image (a) and corresponding SAED image (b).

after calcination at 1,000°C was examined by FESEM. Figure 1a shows FESEM image of the Y₂O₃ phosphor particles codoped with a 1%Eu³⁺-1%Dy³⁺ composition. From the FESEM image, it is apparent that the Y₂O₃:1%Eu³⁺-1%Dy³⁺ phosphor particles consists of relatively uniform, spherical-shaped submicron particles, 100 ± 20 nm in size.

Codoping with different Eu³⁺ and Dy³⁺ concentrations did not alter the morphology of the final phosphor product, and all particles had a spherical morphology with a size distribution of 100 ± 20 nm (not shown for other samples). On the other hand, we showed that the sizes

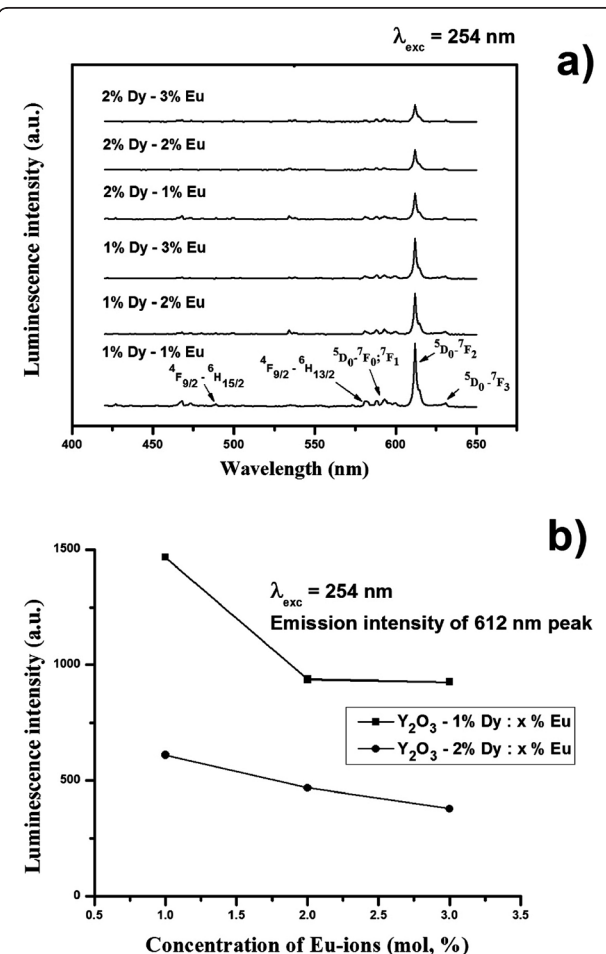
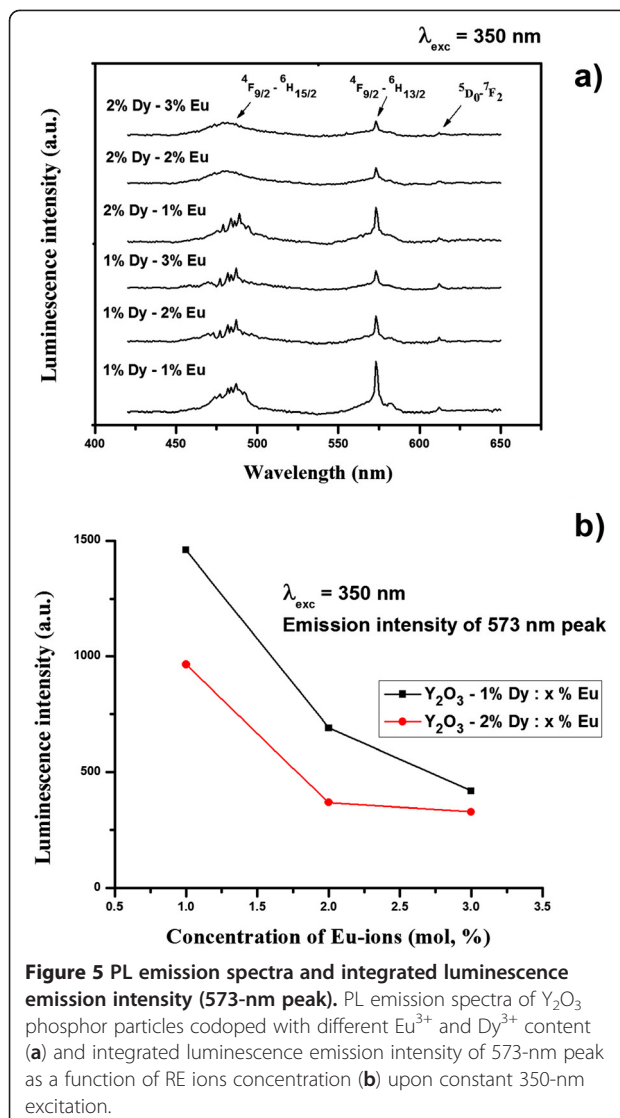


Figure 4 PL emission spectra and integrated luminescence emission intensity (612-nm peak). PL emission spectra of Y₂O₃ phosphor particles codoped with different Eu³⁺ and Dy³⁺ contents (a) and integrated luminescence emission intensity of 612-nm peak as a function of RE ion concentration (b) upon constant 254 nm excitation.



of the final Y_2O_3 phosphor particles can be tuned by altering the reaction time, reaction temperature, and concentration of starting materials [8]. The EDX analysis of 1%Eu³⁺-1%Dy³⁺-codoped Y_2O_3 particles confirmed the presence of dysprosium and europium elements in the yttria host material (Figure 1b). Figure 2 shows the XRD patterns of Y_2O_3 submicron particles codoped with different Eu³⁺ and Dy³⁺ compositions, and the standard peak positions of a pure cubic Y_2O_3 structure (JCPDS No. 86–1107).

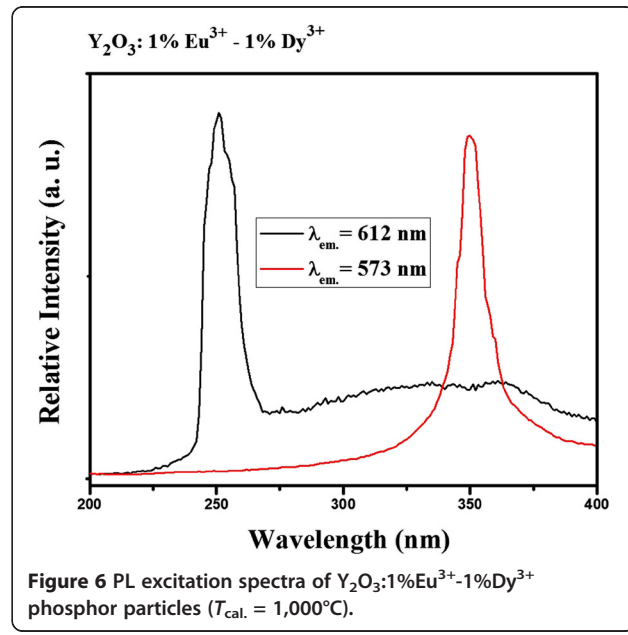
It is obvious that all the diffraction peaks could be indexed directly to the cubic Y_2O_3 phase with the space group $Ia\bar{3}$ (206) according to the standard card (JCPDS No. 86–1107). No additional peaks from the doped components could be detected due to a relatively low concentration of dopant ions indicating the formation of a pure cubic Y_2O_3 phase. Table 1 lists the mean crystallite sizes of synthesized particles estimated from the well-

known Debye-Scherrer's equation. The diffraction data of the three strongest peaks ({222}, {440}, and {622} planes) were used to calculate the mean crystallite sizes. The crystallite sizes showed a slightly increasing tendency, which can be attributed to the effect of the increased dopant concentration [8].

Figure 3a shows a FETEM image of a single Y_2O_3 :1%Eu³⁺-1%Dy³⁺ phosphor particle. It is obvious that a single Y_2O_3 :1%Eu³⁺-1%Dy³⁺ particle has a relatively spherical shape consisting of smaller crystallites (approximately $35 \pm 12 \text{ nm}$) associated with each other, which is in good agreement with that calculated from the XRD patterns using the Debye-Scherrer's equation. The lattice fringes in the FETEM image also confirm the high crystallinity of the phosphor product. Figure 3b shows the corresponding selected area electron diffraction (SAED) image of the Y_2O_3 :1%Eu³⁺-1%Dy³⁺ particle. The clear concentric rings from the inside to outside were indexed directly to the {211}, {222}, {400}, {440}, and {622} planes of cubic Y_2O_3 , demonstrating the highly crystalline nature of the phosphor particles.

Luminescent properties

As we mention, the luminescence emission of phosphor materials depends strongly on the synthetic route, size of the phosphor materials, and concentration of dopant ions. The particle sizes were similar for all Eu³⁺- and Dy³⁺-codoped Y_2O_3 samples which were fabricated under identical conditions. This allows a comparison of the luminescence emission properties of Y_2O_3 phosphor particles codoped with different concentrations of Eu³⁺ and Dy³⁺ activators. Figure 4a shows the emission spectra of Y_2O_3 phosphor particles codoped with different



Eu^{3+} and Dy^{3+} concentrations under ultraviolet (254 nm) irradiation. The emission spectrum showed several main groups of emission lines, which were assigned to the $^5\text{D}_1 \rightarrow ^7\text{F}_1$ and $^5\text{D}_0 \rightarrow ^7\text{F}_j$ (where $j = 0, 1, 2$, and 3) transitions within Eu^{3+} [8,12]. Obviously, the emission spectrum is dominated by a red $^5\text{D}_0 \rightarrow ^7\text{F}_2$ (612 nm) transition within the Eu^{3+} . Figure 4b shows the $^5\text{D}_0 \rightarrow ^7\text{F}_2$ (612 nm) transition peak height as a function of the codoped Eu^{3+} and Dy^{3+} concentration under ultraviolet (254 nm) irradiation. According to the recent literature, the best doping value of Eu^{3+} was reported to be approximately 5 mol% in Y_2O_3 host material [5,13]. On the other hand, the luminescence intensity of the $^5\text{D}_0 \rightarrow ^7\text{F}_2$ (612 nm, hypersensitive to the environment) transition decreased significantly (Figure 4a,b) with increasing codoped Eu^{3+} and Dy^{3+} concentrations in Y_2O_3 host.

Figure 5a shows the same samples under 350-nm excitation. In this case, the emission spectrum exhibited luminescence spectra assigned to the characteristic $^4\text{F}_{9/2} \rightarrow ^6\text{H}_{15/2}$ (blue region) and $^4\text{F}_{9/2} \rightarrow ^6\text{H}_{13/2}$ (greenish-yellow region) transitions within Dy^{3+} [11]. The intensity of the Dy^{3+} characteristic emission transitions also decreased strongly with increasing codoped Eu^{3+} and Dy^{3+} concentration, as it shown in Figure 5a,b. The strong quenching behavior at high codoped Eu^{3+} and Dy^{3+} concentrations was related to a cross-relaxation mechanism (nonradiative decay of the two ions to the ground state) within the dopant ions.

The mean distance between the dopant ions at high concentrations ($R = 0.62/(N)^{1/3}$, where N is the concentration of ions) was much shorter. Therefore, ions can interact through an electric multipolar process leading to energy migration. The dipole-dipole quenching process is inversely proportional to the sixth power of ion-ion separation and, thus, to the square of the dopant concentration [14,15]. In Figures 4a and 5a, except for a

decrease of the luminescence intensity, the emission spectrum of Y_2O_3 particles codoped with different Eu^{3+} and Dy^{3+} concentrations was similar due to the same $f-f$ transitions within the specific RE ion. Therefore, the concentration of codoped RE ions plays an important role and should be strongly considered during the phosphor fabrication process.

The excitation spectra of Y_2O_3 :1% Eu^{3+} -1% Dy^{3+} particles are shown in Figure 6. The excitation spectra of Y_2O_3 :1% Eu^{3+} -1% Dy^{3+} ($\lambda_{\text{em}} = 612$ nm) consists of a band extending from approximately 230 to 260 nm, which is related to the charge-transfer band (CTB) of $\text{O}^{2-}-\text{Eu}^{3+}$ bond. Upon excitation into the CTB at 254 nm, the emission spectrum exhibited several emission lines that were assigned to the $^5\text{D}_1 \rightarrow ^7\text{F}_1$ and $^5\text{D}_0 \rightarrow ^7\text{F}_j$ (where $j = 0, 1, 2$, and 3) transitions within Eu^{3+} , as shown in the Figure 7. On other hand, the weak signal at 573 nm, which was assigned to $^4\text{F}_{9/2} \rightarrow ^6\text{H}_{13/2}$ (hypersensitive transition of Dy^{3+}), was also observed, as shown in Figures 7 and 8. Figure 6 also shows the excitation spectra of Y_2O_3 :1% Eu^{3+} -1% Dy^{3+} particles measured in the 200- to 400-nm range by monitoring the yellow emission transition of Dy^{3+} ($\lambda_{\text{em}} = 573$ nm). In this case, when the excitation wavelength was switched to 350 nm, the hypersensitive $^6\text{P}_{7/2}$ level of Dy^{3+} was excited resonantly, which then quickly relaxes nonradiatively to populate the $^4\text{F}_{9/2}$ level [11]. Radiative emission occurred from $^4\text{F}_{9/2}$ to a lower $^6\text{H}_{15/2}$ and $^6\text{H}_{13/2}$, emitting at 488 and 573 nm, respectively, with feeble ET to Eu^{3+} . The energy transferred to Eu^{3+} cascades rapidly via nonradiative transitions to the $^5\text{D}_0$ state, from which luminescence associated with Eu^{3+} occurs. Therefore, the feeble signal of the $^5\text{D}_0 \rightarrow ^7\text{F}_2$ (612 nm) transition within Eu^{3+} was also detected in Eu^{3+} and Dy^{3+} codoped phosphor particles upon 350-nm excitation.

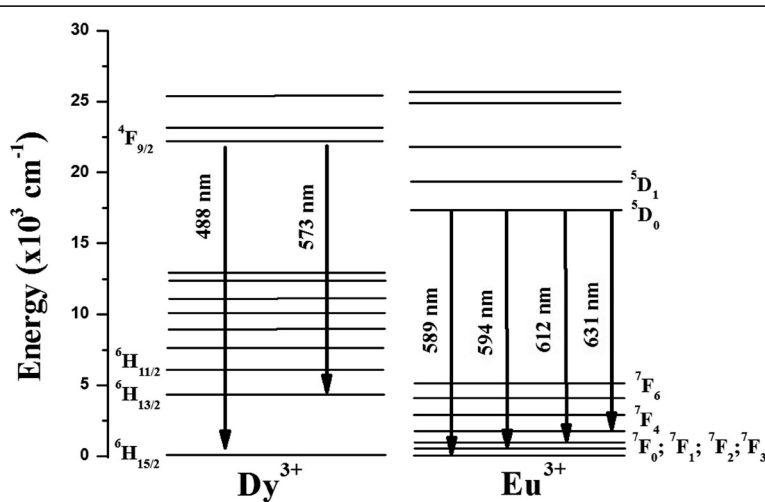


Figure 7 Schematic diagram illustrating the $\text{Dy}^{3+}/\text{Eu}^{3+}$ energy level diagram and transitions between the levels.

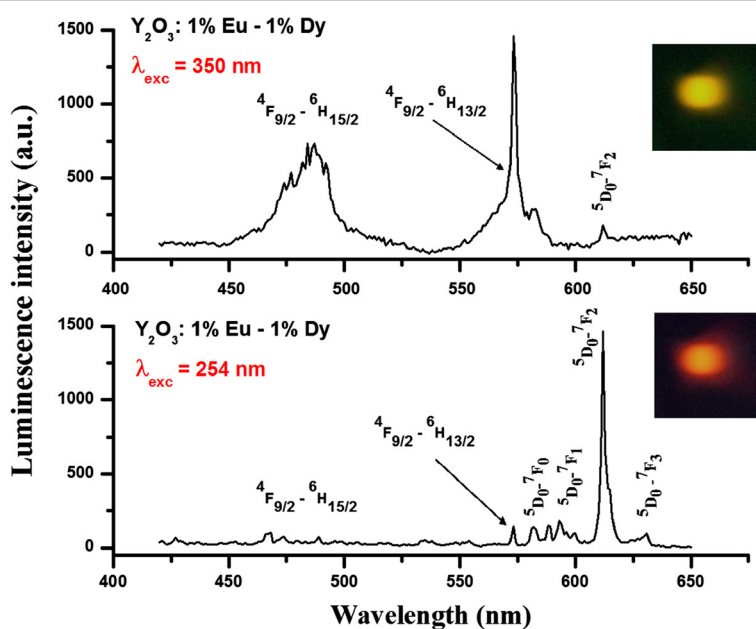


Figure 8 PL emission spectra of Y_2O_3 :1% Eu^{3+} -1% Dy^{3+} phosphor particles ($\lambda_{\text{exc.}} = 254$ and 350 nm, respectively) with assigned transitions. Inset digital photographs showed the eye-visible red and yellow luminescence emissions.

Such behavior suggests that there is some energy transfer (ET) occurring between the two codoped ions. On the other hand, the ET observed in Eu^{3+} - and Dy^{3+} -codoped Y_2O_3 was not as strong as that observed in Tb^{3+} - Eu^{3+} -codoped Y_2O_3 phosphor [8]. Therefore, the emission wavelength and color output of the same Y_2O_3 :1% Eu^{3+} -1% Dy^{3+} particles can be adjusted by switching the radiation from 254 to 350 nm. The digital photographs of eye-visible luminescence emissions from Y_2O_3 :1% Eu^{3+} -1% Dy^{3+} particles upon 254 and 350 nm excitations are shown in the Figure 8. It is obvious that the same host material emit red or yellow color, depending on the excitation wavelength.

Conclusion

In conclusion, Eu^{3+} - and Dy^{3+} -codoped Y_2O_3 submicron spherical particles were synthesized using the urea homogeneous precipitation method. The crystal structure and morphology of synthesized particles were characterized by XRD, FESEM, EDX, and FETEM. The PL spectroscopy was used to examine luminescent properties of Eu^{3+} - and Dy^{3+} -codoped Y_2O_3 particles. PL measurements revealed strong concentration quenching at high-codoped Eu^{3+} and Dy^{3+} concentrations. The luminescence color emission could be controlled by the excitation wavelength and the incorporation of Dy^{3+} and Eu^{3+} at the appropriate concentrations into Y_2O_3 structure. Weak energy transfer between the codoped ions was observed. These color-tunable Y_2O_3 :1% Eu^{3+} -1% Dy^{3+}

phosphor particles can be used for security printing, solid state illumination, or for optical displays.

Competing interests

The authors declare that they have no competing interests.

Authors' contributions

All the specimens used in this study and initial manuscript were prepared by TSA. YHH and HKK added a valuable discussion and coordinated the present study as principal investigators. All authors read and approved the final manuscript.

Acknowledgments

This work was supported by the National Research Foundation of Korea (NRF) funded by the Ministry of Education, Science and Technology (grant no.: 2010-0010575) and by the Korean government (grant no. 2012R1A1B3001357). The author would like to thank Prof. J. B. Lee for allowing the use of his equipment for the preparation and characterization of the samples.

Received: 9 July 2012 Accepted: 21 September 2012

Published: 8 October 2012

References

1. Das GK, Tan TTY: Rare-earth-doped and codoped Y_2O_3 nanomaterials as potential bioimaging probes. *J Phys Chem C* 2008, **112**:11211–11217.
2. Yang P, Gai S, Liu Y, Wang W, Li C, Lin J: Uniform hollow Lu_2O_3 :Ln (Ln = Eu^{3+} , Tb^{3+}) spheres: facile synthesis and luminescent properties. *Inorg Chem* 2011, **50**:2182–2190.
3. Qin X, Yokomori T, Ju Y: Flame synthesis and characterization of rare-earth (Er^{3+} , Ho^{3+} , and Tm^{3+}) doped upconversion nanophosphors. *Appl Phys Lett* 2007, **90**:073104.
4. Tu D, Liang Y, Liu R, Li D: Eu/Tb ions co-doped white light luminescence Y_2O_3 phosphors. *J Lumin* 2011, **131**:2569–2573.
5. Wang H, Yang J, Zhang CM, Lin J: Synthesis and characterization of monodisperse spherical SiO_2 @ RE_2O_3 (RE = rare earth elements) and SiO_2 @ Gd_2O_3 :Ln3+ (Ln = Eu, Tb, Dy, Sm, Er, Ho) particles with core-shell structure. *J Solid State Chem* 2009, **182**:2716–2724.

6. Atabaev TS, Vu H-HT, Piao Z, Kim H-K, Hwang Y-H: Tailoring the luminescent properties of codoped $\text{Gd}_2\text{O}_3:\text{Tb}^{3+}$ phosphor particles by codoping with Al^{3+} ions. *J Alloys Compd* 2012, **541**:263–268.
7. Flores-Gonzales MA, Ledoux G, Roux S, Lebbou K, Perriat P, Tillement O: Preparing nanometer scaled Tb-doped Y_2O_3 luminescent powders by the polyol method. *J Solid State Chem* 2005, **178**:989–997.
8. Atabaev TS, Lee JH, Han DW, Hwang Y-H, Kim H-K: Cytotoxicity and cell imaging potentials of submicron color-tunable yttria particles. *J Biomed Mat Res A* 2012, **100**(9):2287–2294.
9. Ishiwada N, Fujioka S, Ueda T, Yokomori T: Co-doped $\text{Y}_2\text{O}_3:\text{Tb}^{3+}/\text{Tm}^{3+}$ multicolor emitting phosphors for thermometry. *Opt Lett* 2011, **36**:5.
10. Cheng B, Zhang Z, Han Z, Xiao Y, Lei S: $\text{SrAl}_2\text{O}_4:\text{Eu}^{2+}, \text{Dy}^{3+}$ nanobelts: synthesis by combustion and properties of long-persistent phosphorescence. *J Mater Res* 2011, **26**:2311–2315.
11. Atabaev TS, Vu HHT, Kim H-K, Hwang Y-H: Synthesis and optical properties of Dy^{3+} -doped Y_2O_3 nanoparticles. *J Korean Phys Soc* 2012, **60**:244–248.
12. Seo S, Yang H, Holloway P: Controlled shape growth of Eu- or Tb-doped luminescent Gd_2O_3 colloidal nanocrystals. *J Colloid Interface Sci* 2009, **331**:236–242.
13. Liu Z, Yu L, Wang Q, Tao Y, Yang H: Effect of Eu, Tb codoping on the luminescent properties of Y_2O_3 nanorods. *J Lumin* 2011, **131**:12–16.
14. Atabaev TS, Vu H-HT, Kim YD, Lee JH, Kim H-K, Hwang Y-H: Synthesis and luminescence properties of Ho^{3+} doped Y_2O_3 submicron particles. *J Phys Chem Solids* 2012, **73**:176–181.
15. Patra A, Ghosh P, Chowdhury PS, Alencar MARC, Lozano W, Rakov N, Maciel GS: Red to blue tunable upconversion in Tm^{3+} -doped ZrO_2 nanocrystals. *J Phys Chem B* 2005, **109**:10142–10146.

doi:10.1186/1556-276X-7-556

Cite this article as: Atabaev et al.: Color-tunable properties of Eu^{3+} - and Dy^{3+} -codoped Y_2O_3 phosphor particles. *Nanoscale Research Letters* 2012 **7**:556.

Submit your manuscript to a SpringerOpen® journal and benefit from:

- Convenient online submission
- Rigorous peer review
- Immediate publication on acceptance
- Open access: articles freely available online
- High visibility within the field
- Retaining the copyright to your article

Submit your next manuscript at ► springeropen.com